Journal of Materials Chemistry A

COMMUNICATION

View Article Online
View Journal | View Issue

Cite this: J. Mater. Chem. A, 2014, 2, 17272

Received 2nd August 2014
Accepted 28th August 2014

DOI: 10.1039/c4ta03983a

www.rsc.org/MaterialsA

Conjugated polymer composite artificial muscle with solvent-induced anisotropic mechanical actuation†

Xin Lu, Zhitao Zhang, Houpu Li, Xuemei Sun* and Huisheng Peng*

Responsive polymers have been widely studied as actuators in response to external stimuli and exhibit promising applications in wide variety of fields. However, the actuating direction of most polymers cannot be precisely controlled, and the generated low stress and poor stability cannot meet practical applications either. Herein, conjugated polymer/aligned multi-walled carbon nanotube (MWCNT) composites are designed, which can undergo anisotropic and reversible bending/unbending actuations driven by solvents. The actuating direction was accurately controlled to be perpendicular to the MWCNT length, which is realized through the orientation of conjugated polymers induced by aligned MWCNTs. The actuation generates a stress of 15 MPa, approximately 42 times of the strongest human muscle, and the reversible actuations are repeated for 300 cycles without fatigue. These composite artificial muscles can be widely used in numerous fields, such as sensors and actuators.

Introduction

Responsive polymers can reversibly change their shapes, sizes and colors in response to external stimuli such as electricity, light, heat, pH, biomolecule and solvent, which enable promising applications in a wide variety of fields including optoelectronic devices, smart windows, electric motors, sensors and compressors.[1–6] Among them, solvent-responsive polymers including hydrogels and liquid crystal polymer gels driven by water and conducting polymers driven by solvent or vapor gradients are significantly investigated.[7–10] For over half a century, polymer hydrogels are widely demonstrated with large strains, but their applications are hindered because of the contradiction between mechanical stability and response rate, as well as low generated stress.[7,8,11] In most of the cases, these hydrogels also deliver an isotropic expansion and contraction. Liquid crystal polymers are controlled to exhibit anisotropic actuations through the molecule orientation made by mechanical rubbing.[12] However, their mechanical properties are poor due to the production of damaged structures during preparation, and low stabilities in use.[13–15]

For conducting polymers, such as poly (diphenylacetylene) derivatives, the solvent driven actuation was generated due to the volume change of polymers caused by the uptake and release of solvents.[16,17] They show extremely large fractional free volumes due to the stiff backbones and steric repulsions of substituents.[18,19] Consequently, gases and organic solvents can readily diffuse into these polymers to change the molecular distances and solid-state electronic structures, resulting in the change of volume and enhancement of fluorescence.[20,21] The swelling-induced emission enhancement of these polymers has been widely studied for fluorescent optical sensors in response to solvents. However, the capability for obvious volume changes has been explored little for sensors such as solvent-driven actuators.[19,22] In addition, most of the fluorescence and volume change of these polymers were isotropic due to the non-directional arrangement of main chains. Therefore, it still remains a challenge to make poly (diphenylacetylene) derivative actuators with controlled actuating directions in response to solvents. Thus, the conjugated backbones are required to be effectively oriented with an anisotropic geometry.

In addition, carbon nanotubes can be combined with conjugated polymers to enhance their electrical, mechanical and optical properties.[23–25] For instance, polyacetylene chain can interact with and get wrapped around carbon nanotubes in solution because of the strong π–π interactions between the carbon nanotubes and polymers.[26,27] However, the filled carbon nanotubes are typically randomly dispersed in polymer matrices, and the resulting polymer composite materials exhibit limited mechanical strengths and electrical conductivities. To further improve their practical applications, it is necessary to assemble carbon nanotubes into highly aligned

State Key Laboratory of Molecular Engineering of Polymers, Department of Macromolecular Science and Laboratory of Advanced Materials, Fudan University, Shanghai 200438, China. E-mail: sunxm@fudan.edu.cn; penghs@fudan.edu.cn

† Electronic supplementary information (ESI) available. See DOI: 10.1039/c4ta03983a

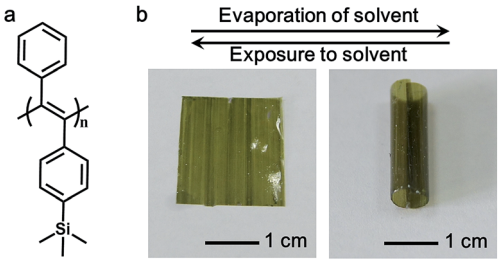

Fig. 1 (a) Molecular structure of PTP. (b) Images of a bilayer composite film being rolled and recovered on evaporation and absorption of ethanol, respectively.

structures to effectively extend the remarkable properties from nanoscale to macroscopic scale.[28–32]

Herein, we have synthesized a new conjugated polymer composite film by spin-coating a poly [1-phenyl-2-(*p*-trimethylsilyl) phenylacetylene] (PTP, Fig. 1a) solution, a representative poly (diphenylacetylene) derivative, onto aligned multi-walled carbon nanotube (MWCNT) sheets. An actuator was made in a bilayer form with an anisotropic MWCNT/PTP composite layer being deposited on an isotropic substrate. Strong π–π interactions were discovered between PTP and MWCNT mainly through side phenyl groups of PTP and side walls of MWCNT.[27] The conjugated polymer chains were oriented by the aligned MWCNTs, thus the change of inter-chain distances typically occurs in the direction perpendicular to the MWCNT length. Therefore, the bilayer composite films exhibited anisotropic bending and unbending deformations with controlled direction along the perpendicular direction relative to the MWCNT length, *e.g.*, rolling into a tube and recovering to a flat format under stimulation by organic solvents (Fig. 1b). The synergetic interactions between MWCNTs and PTP have also greatly improved the mechanical strength and the stability of the composite actuators, which can be repeatedly deformed for 300 cycles. The use of these as a miniature crane and a micro-valve has been demonstrated. Artificial flowers based on these aligned MWCNT/PTP composite films on poly (dimethylsiloxane) substrate have also been developed to reversibly open and close, mimicking the leaf of Venus flytrap.

Experimental section

Materials

The precursor of poly (dimethylsiloxane), Sylgard 184, was obtained from Dow Corning. Ethanol (purity ≥ 99.7%) and *n*-hexane (purity > 97.0%) were obtained from Sinapharm Chemical Reagent Co., Ltd. Methanol (purity > 99.5%) was obtained from Shanghai Lingfeng Chemical Reagent Co., Ltd. All the chemicals were used as received without further purification.

Preparation of aligned MWCNT and PTP

MWCNT arrays were synthesized by chemical vapor deposition at 740 °C with Fe (1 nm)/Al_2O_3 (10 nm) on a silicon substrate as the catalyst, ethylene as the carbon source and a mixture of Ar and H_2 as the carrier gas. The flow rates of C_2H_4, Ar, and H_2 were 90, 400, and 30 sccm, respectively.[24,30] Aligned MWCNT sheets were directly spun from the array. Generally, one layer of the sheets showed a thickness of ~20 nm, and they could be stacked into thicker sheets along the stacking direction. In this work, MWCNT arrays with heights of ~250 μm were mainly used. PTP was synthesized by polymerizing the monomer, trimethyl[4-(phenylethynyl)phenyl]-silane, and the synthetic details are described elsewhere.[31,32]

Preparation of aligned MWCNT/PTP composite films

Poly (dimethylsiloxane) substrate with a thickness of 120 μm was prepared using Sylgard 184. Generally, poly (dimethylsiloxane) precursor was cast onto a glass slide and then thermally cured at 80 °C for 2 h. The aligned MWCNT sheets were dry-drawn from the MWCNT array and transferred onto the poly (dimethylsiloxane) substrate. The PTP/toluene solution (concentration of 1.5 mg mL^{-1}) was spin-coated onto the aligned MWCNTs with rotation rates of 1000 rpm for 15 s and then 1500 rpm for 20 s. The preparation process and the structure of the composite film are schematically shown in Fig. S1.† The content of PTP can be controlled by varying the coating times and the concentration of the solution. The aligned MWCNT/PTP composite film on the poly (dimethylsiloxane) or poly (ethylene terephthalate) was removed from the glass slide and cut into square samples having the same width of 2 cm.

Characterization

The structures of aligned MWCNT sheets and MWCNT/PTP composite films were characterized by scanning electron microscope (SEM, Hitachi FE-SEM S-4800, operated at 1 kV). To obtain the image from a top view, the composite film was placed on a sample stage with the MWCNT/PTP layer at the top. The cross-sectional image was obtained by cutting the film and then observing it from the side. Small-angle X-ray scattering (SAXS) patterns were obtained using a Nanostar U SAXS system (Bruker, Germany) equipped with a Cu Kα radiation source. The thicknesses of aligned MWCNT/PTP composite films were measured using a Dektak 150 surface profilometer. UV-vis and fluorescence measurements were performed on Shimadzu UV-2550 and Shimadzu-RF5301PC (with an excitation wavelength of 370 nm) spectroscope, respectively. During the UV-vis measurement, a bare PTP film was prepared by spin-coating the PTP/toluene solution (concentration of 1.5 mg mL^{-1}). The stacked film was prepared by attaching an MWCNT sheet onto PTP film (labeled as "MWCNT + PTP film"). Both composite and stacked films were prepared under the same conditions, including the same aligned MWCNT sheet with weight percentage of ~55.0%, thickness of ~40 nm and density of 2.8 μg cm^{-2}. The randomly dispersed MWCNT film was also prepared through a spin-coating process with a thickness of ~40 nm. Raman measurements were made with a Renishaw inVia Reflex Raman spectroscopy system with an excitation wavelength of 632.8 nm. The PTP content was determined by

thermogravimetric analysis (Shimadzu DTG-60H) in air. The X-ray diffraction pattern was obtained using a D8 Advance and Davinci. Design diffractometer (Bruker) equipped with a Cu Kα radiation source (wavelength of 1.54 Å) operated at 35 kV and 30 mA. The electrical conductivity was measured by a two-probe method through a Keithley Model 2400 source meter. Mechanical measurements were performed on a Hengyi Table-Top universal testing instrument. The composite films were mounted onto sample holders with a gauge length of 5 mm. The samples used for measurements of the generated force were exactly 17.3 mm × 2.5 mm × 595 nm. Ethanol was added to the top clamp and flowed down to diffuse into the composite film and the force was recorded over time during absorption and evaporation of solvent (Fig. S2†).

Results and discussion

MWCNT arrays that can spin, are first synthesized by chemical vapor deposition,[30,33] and aligned MWCNT sheets are then dry-drawn from the array and stabilized on the poly (dimethylsiloxane) or poly (ethylene terephthalate) substrate. The thicknesses of MWCNT sheets can be appropriately controlled from 20 nanometers to several micrometers as required. Fig. 2a shows a typical scanning electron microscopy (SEM) image of a bare aligned MWCNT sheet with voids ranging from tens to hundreds of nanometers. The high alignment is further confirmed by a pair of dense reflection areas in the horizontal direction in the two-dimensional small-angle X-ray scattering pattern (Fig. S3†).Then, polymer solution can be coated onto the aligned MWCNT sheet to prepare composite materials.[28,34] PTP (Fig. 1a) is synthesized after polymerization of the monomer, *i.e.*, trimethyl[4-(phenylethynyl)phenyl]-silane.[31] The average molecular weight and polydispersity index of PTP are 5.46×10^6 and 1.43, respectively. The composite film had been prepared by spin-coating a PTP solution onto the aligned MWCNT sheet that was placed on a poly (dimethylsiloxane) or poly (ethylene terephthalate) substrate. Fig. 2b shows an SEM image of the MWCNT/PTP composite film from a top view, indicating that the PTP infiltrates the voids among the aligned MWCNTs. Notably, the MWCNTs maintain the highly aligned structure in the MWCNT/PTP composite film, similar to the bare aligned MWCNT sheets. Fig. 2c and d show SEM images of the side view of a bilayer composite film. The top layer of aligned MWCNT/PTP composite demonstrates a thickness of ~400 nm, which is verified by a Dektak 150 surface profilometer (Fig. S4†).

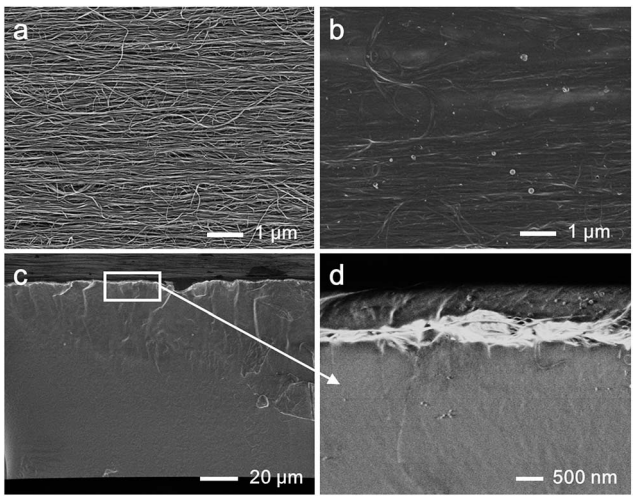

Fig. 2 SEM images. (a) A bare aligned MWCNT sheet. (b) Top view of an aligned MWCNT/PTP composite film. (c and d) Side views of the bilayer film of an aligned MWCNT/PTP composite film on a poly (dimethylsiloxane) substrate at low and high magnifications, respectively.

The aligned MWCNT/PTP composite films exhibit high tensile strengths and electrical conductivities of 250–500 MPa and 300–400 S cm^{-1} at room temperature, respectively. Fig. 3a shows a typical stress–strain curve of the aligned MWCNT/PTP composite film at the MWCNT weight percentage of ~30% with a tensile strength of ~290 MPa, whereas a bare PTP film exhibited a tensile strength of only 16.5 MPa (Fig. S5†). The strength can be further enhanced by increasing the weight percentage of MWCNTs, *e.g.*, ~470 MPa at ~60% (Fig. S6†). Fig. 3b further traces the forces generated from the composite film in response to solvent. When the composite film was exposed to ethanol, the force showed a sharp fluctuation because of the sudden drop of ethanol; the force was then decreased because of the PTP swelling; the force finally increased due to the PTP contraction during the evaporation of ethanol. During transition from swelling to contracting states, the films produce a force of 0.0223 N with a stress of ~15 MPa, compared with 0.35 MPa for the strongest human muscle, less than 1 MPa for polymer gels and 1–8 MPa for elastomers.[15,35] Although the stresses that are generated from electroactive conducting and ionic polymers were comparable to those from the aligned MWCNT/PTP composite film, conducting and ionic polymers exhibited much lower tensile strengths.[36,37] Therefore, the aligned MWCNT/PTP composite films may represent a new family of materials for artificial muscles.

The reversible mechanical actuation based on solvent was further quantitatively studied based on a square bilayer composite film with a width of 2 cm (Fig. 3c). Fig. 3d shows the change in width between the two edges of a bilayer composite film over 300 bending/unbending cycles. This distance between the two edges was used to trace the deformable reversibility, and the square bilayer composite film with PTP weight percentage of ~57.5% in MWCNT/PTP active layer was demonstrated. Obviously, this anisotropic bending deformation of the bilayer composite film is reversible for at least 300 cycles, and the bending direction is always perpendicular to the MWCNT length.

Two important factors were found to affect the bending capability of the bilayer composite film, *i.e.*, weight percentage of PTP in the MWCNT/PTP composite film and absorption/evaporation speed of the solvent. Fig. 3e shows the change in the width as a function of the PTP weight percentage in the composite film. The width remained almost unchanged at PTP weight percentages less than 40% because the force generated from the PTP contraction was not sufficiently high to induce the deformation of the poly (dimethylsiloxane) substrate. Beyond

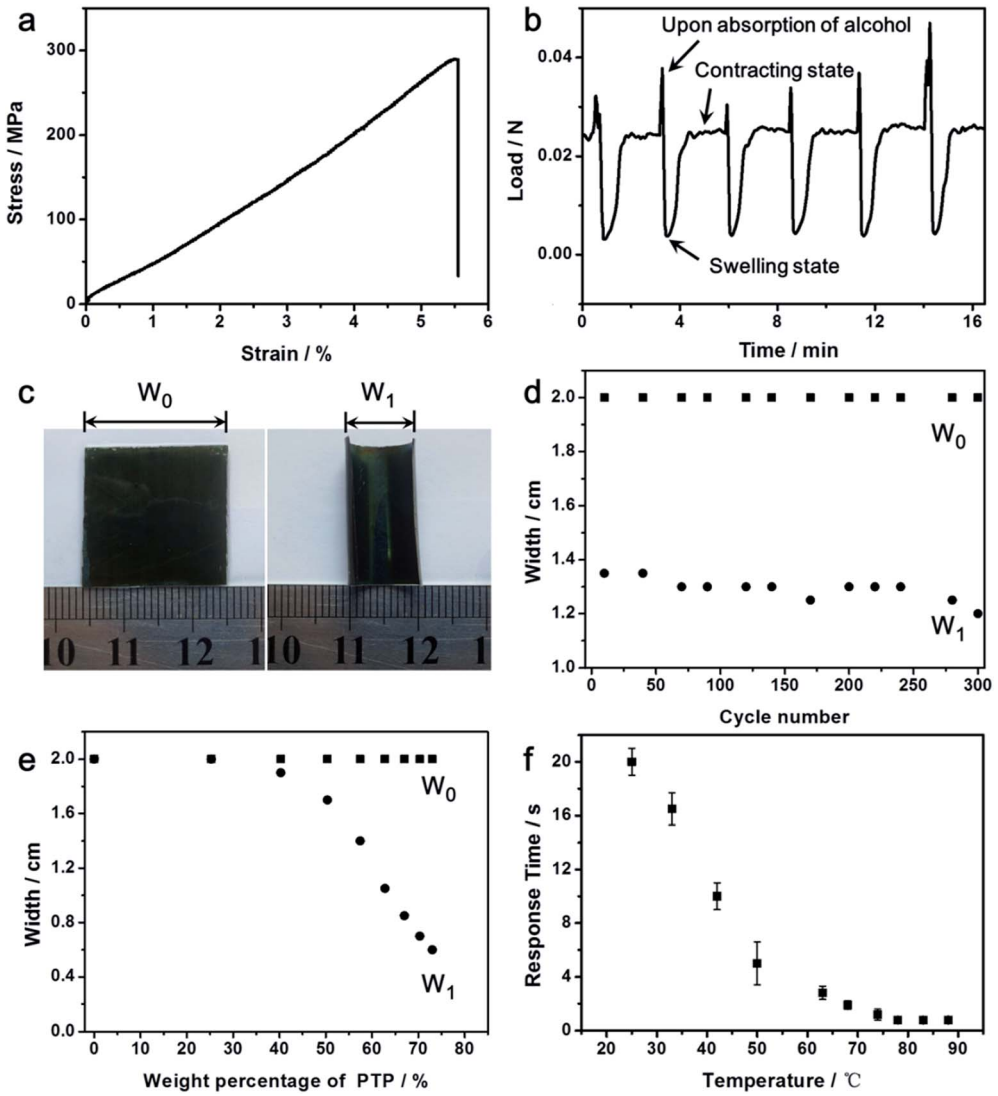

Fig. 3 Mechanical and solvomechanical actuating properties of composite films. (a) A typical stress–strain curve of an aligned MWCNT/PTP composite film with an MWCNT weight percentage of ~30%. (b) Variation of the force generated from the aligned MWCNT/PTP composite film with a MWCNT weight percentage of ~30% upon absorption and evaporation of ethanol. (c) Images of two representative shapes of the bilayer composite film during the reversible bending and unbending processes caused by the evaporation and absorption of ethanol. (d) Dependence of width on cycle number. (e) Dependence of the width on the weight percentage of PTP. (f) Dependence of response time on temperature. W_0 and W_1 correspond to the widths between the two opposite edges of the composite film before and after evaporating ethanol, respectively.

this critical point, the increased forces made the film to bend and the width after bending was decreased with increasing PTP weight percentage. For example, the bilayer composite films with PTP weight percentages of ~57.5% and ~62% in the MWCNT/PTP layer were bent into curved structures with the edge distances of ~1.3 and ~1.0 cm, respectively. When the weight percentage of PTP was higher than 83%, the bilayer composite film even rolled into a tube with a higher curvature (Fig. 1b). For a composite film that can roll into a tube, the swelling ratio of the MWCNT/PTP composite film in a direction perpendicular to the MWCNT length was estimated to be 1.2% with respect to the width and thickness of the composite film. The bending rate was determined by the evaporation speed of ethanol that may be studied by varying the temperature. For a typical square composite film with width of 2 cm, it takes ~20 s to fully bend into a curved structure at room temperature. A higher temperature increased the evaporation speed of ethanol with a more rapid bending (Fig. 3f). When the temperature was equal to or higher than the boiling point of ethanol, the bending was completed in ~0.6 s (Movie S1†). The unbending processes were completed in less than 1 s on absorbing ethanol.

Conjugated polymers with high molecular weights and rigid chains can be easily oriented by a shear force.[22,38] Here, no external shearing forces were used during the preparation of the PTP. Therefore, the alignment of MWCNTs and their interactions with the PTP should contribute to the anisotropic bending of the composite film. UV-vis and fluorescent spectroscopy were performed to investigate the interactions between the aligned

MWCNTs and PTP.[27,39] A control sample of a stacked film was prepared by simply attaching an aligned MWCNT sheet onto PTP film. Fig. 4a compares the UV-vis spectra of aligned MWCNT sheet, bare PTP, aligned MWCNT/PTP composite film and the stacked film. The peaks at ~375 nm and ~425 nm are attributed to the π–π* transition of localized electrons in PTP in a direction perpendicular and parallel to the backbone, respectively.[40] The ratio of the two absorption bands (A_{425}/A_{375}) of aligned MWCNT/PTP composite film (1.10) was slightly higher than that of the stacked film of aligned MWCNT sheet on PTP (0.98), elucidating a synergetic interaction between the aligned MWCNTs and PTP.[41] In contrast, the ratio of the randomly dispersed MWCNT/PTP composite, *i.e.*, 1.14, was close to 1.12 of the stacked MWCNT on PTP film (Fig. S7a†). It should be noted that for the investigated thickness range of PTP film, the A_{425}/A_{375} values remained almost unchanged, although the absorption intensities were increased with increasing thickness (Fig. S7b†). In addition, the fluorescent intensity of aligned MWCNT/PTP composite film was considerably lower, and the emission band shifted to a longer wavelength compared with bare PTP and the stacked film under the same conditions, indicating an effective emission quenching caused because of the increase in the degree of intramolecular phenyl–phenyl stacking and the electron or energy transfer between the aligned MWCNT and PTP (Fig. 4b).[19]

Raman spectroscopy was also used to study the MWCNT/PTP interactions and orientations of PTP backbones (Fig. 5a).[25,39] After the formation of the composite film, the characteristic Raman peaks of bare MWCNTs at 1577 and 2649 cm^{-1} shifted to higher wavenumbers of 1579 and 2652 cm^{-1}, respectively, whereas the characteristic peaks of PTP at 545 and 1556 cm^{-1} shifted to lower wavenumbers of 542 and 1553 cm^{-1}, respectively. Therefore, a strong molecular interaction obviously exists between MWCNT and PTP.[42] Raman intensities of PTP in the composite and bare films were further measured with polarized excitation lights in different directions with respect to the MWCNT length (Fig. 5b and c). Raman intensities at ~1553 cm^{-1} that was assigned to the stretching vibration of –C=C– in the PTP main chain decreased with increasing polarization angles from 0° to 90° (Fig. 5d). The dichroic ratio (R) was calculated to be 2.5 by $R = I_{0°}/I_{90°}$, where $I_{0°}$ and $I_{90°}$ correspond to the Raman intensity of the characteristic peak at directions being parallel and perpendicular to the MWCNT length, respectively. Therefore, the aligned structure of MWCNTs induces the orientation of PTP conjugated backbones.[30] In contrast, no obvious change in the Raman intensity of the bare PTP film was observed at different polarization angles.

To better understand the anisotropic bending, the behaviors of six control samples (Fig. S8†) were compared on absorption and evaporation of ethanol. Sample #1 was a bare poly (dimethylsiloxane) substrate which exhibited no bending behavior at all. Sample #2 was prepared by placing an aligned MWCNT sheet onto a poly (dimethylsiloxane) substrate without PTP. This MWCNT/poly (dimethylsiloxane) film was slightly bent along the direction parallel to the MWCNT length because of the stress produced from MWCNTs during drying. However, Sample #2 was bent away from the side of MWCNT sheet, and the bent film cannot be restored by rewetting the film with ethanol. Sample #3 was prepared by spin-coating a PTP solution onto the poly (dimethylsiloxane) substrate without an aligned MWCNT sheet, Sample #4 was prepared by sequentially coating a PTP film and aligned MWCNT sheet on the poly (dimethylsiloxane) film, where PTP and MWCNT exhibited limited contact on surface, and Sample #5 was prepared by coating an MWCNT/PTP mixture dispersion onto the poly (dimethylsiloxane) substrate to form a randomly dispersed MWCNT/PTP composite film. No anisotropic bending was observed from the composite films of Samples #3–5, though a slight astatic crumpling at the edge occurred, when the solvent was evaporated. All the samples were prepared by the same solution of PTP and Samples #2–5 have similar MWCNT contents. Therefore, the orientation of PTP backbones induced by the aligned MWCNTs and strong interactions between them are critical for the anisotropic, reversible bending and unbending actuation. In addition, Sample #6 was prepared by coating other general polymers such as polymethyl methacrylate (PMMA) solution onto the aligned MWCNT on poly (dimethylsiloxane) substrate. This bilayer composite film showed no response to ethanol because PMMA hardly absorbs ethanol to swell.

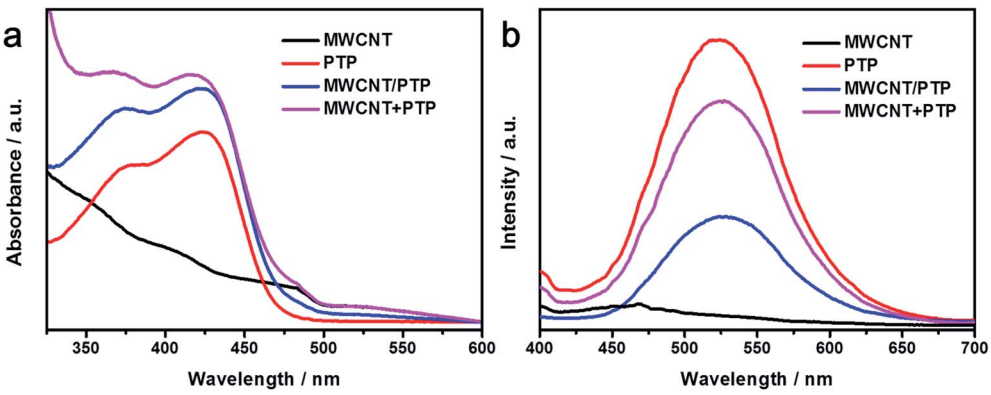

Fig. 4 Interactions between the aligned MWCNT and PTP characterized by (a) UV-vis spectra and (b) fluorescent spectra of PTP film, aligned MWCNT sheet, aligned MWCNT/PTP composite film and stacked aligned MWCNT sheet onto PTP film.

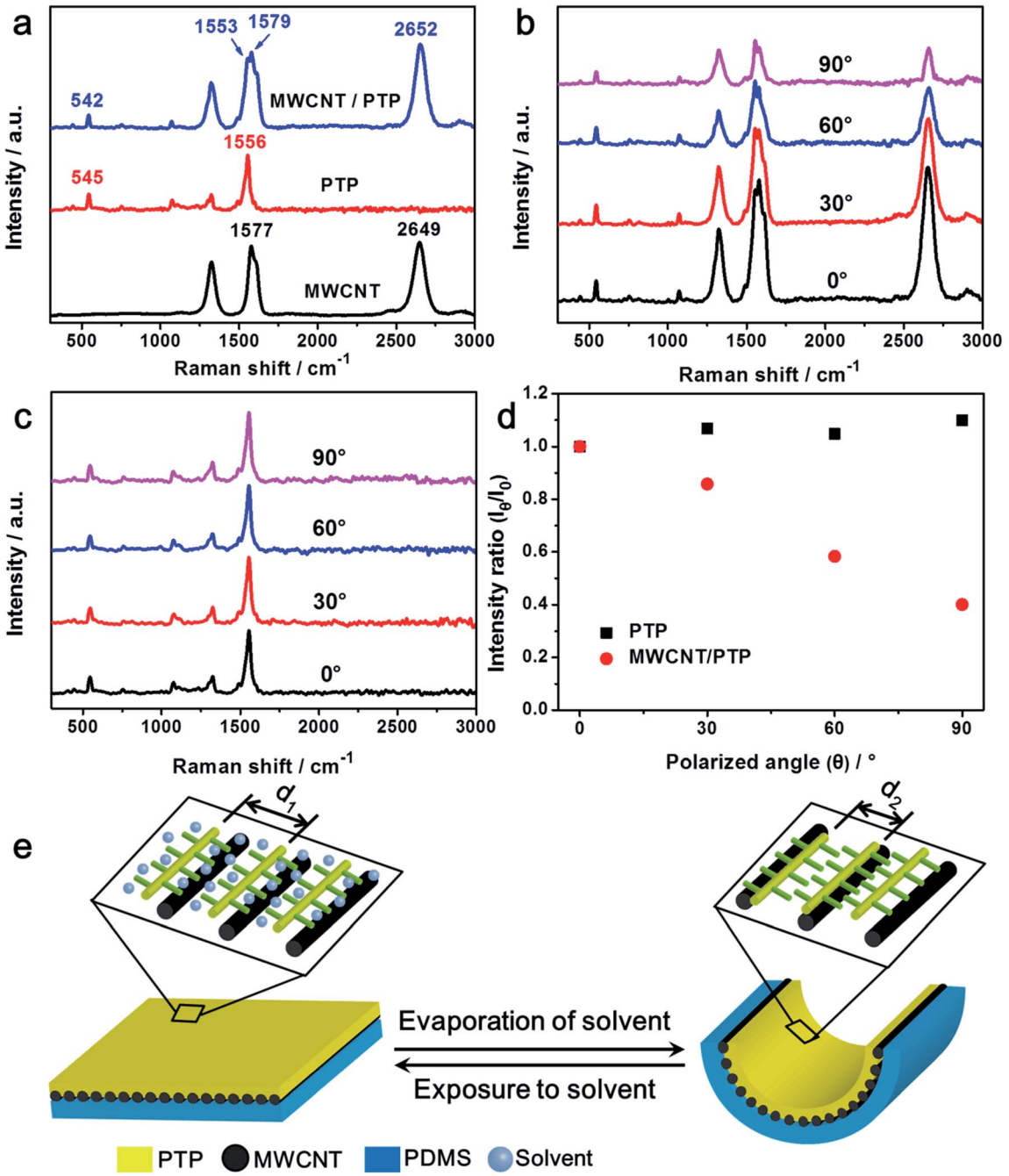

Fig. 5 Mechanism study of the solvomechanical actuation. (a) Raman spectra of an aligned MWCNT/PTP composite film, a PTP film, and a bare MWCNT sheet. (b) Polarized Raman spectra of an aligned MWCNT/PTP composite film. (c) Polarized Raman spectra of a bare PTP film. (d) Dependence of the Raman intensity ratio on the polarization angle for an aligned MWCNT/PTP composite film and for a bare PTP film. (e) Schematic illustration to the bending and unbending behavior of the aligned MWCNT/PTP composite film on the poly (dimethylsiloxane) substrate caused by the absorption and evaporation of ethanol. The inter-chain distances are reduced from d_1 to d_2 after evaporation of solvent.

The reversible deformation may be explained by the reversible re-organization of polymer backbones with different inter-chain distances, *i.e.*, the removal of the solvent induced the backbones to be stacked more closely, while the diffusion of the solvent reversed the process through a hydrophilic–hydrophobic repulsion.[19,43,44] For the bilayer film with MWCNT/PTP composite film on the poly (dimethylsiloxane) substrate, the aligned MWCNTs may induce PTP backbones to orient in a direction parallel to the MWCNT length mainly through π–π interactions. The as-formed lamellar distance of the PTP was ~1.3 nm according to the results of X-ray diffraction (Fig. S9†), and the PTP backbones were swollen to a disordered structure due to the absorption of ethanol. These phenomena were verified by the change in fluorescence before and after the evaporation of ethanol (Fig. S10†). The fluorescent intensity of the aligned MWCNT/PTP composite films largely increased and the

emission band simultaneously shifted to a shorter wavelength, when the films were exposed to ethanol due to the swelling-induced emission enhancement of PTP derived from the change of stack structure in polymer chain.[19,40] Therefore, when the ethanol was evaporated, the PTP at the top composite layer contracted in the direction perpendicular to the MWCNT length, whereas the underlying poly (dimethylsiloxane) layer remained unchanged. As a result, the film curled along the contracted direction (Fig. 5e). The bending rate depends on the rate of evaporation of solvent from the composite film, which in turn depends on the media temperature (Fig. 3f). On absorption of ethanol, the PTP expanded to its original state and the film reversibly returned to its previous morphology. Note that the unbending process was completed more rapidly at room temperature due to the faster diffusion of ethanol into the PTP. The reversible fluorescent change in Fig. S10† can also be repeated for hundreds of cycles, which provides the composite films as the promising solvent sensors and indicators.

It should be noted that the other solvents such as *n*-hexane and methanol can also permeate into the PTP and induce the deformation and fluorescence change of the composite film, while water cannot drive the backbone for a re-organization due to the extremely high polarity and surface tension (Fig. S11 and S12†). This behavior is related to the presence of molecular-scale voids and affinity of PTP to solvent. The micro-voids provided the effective diffusion path for solvent. The solvents with similar solubility parameter values can interact with PTP, resulting in solvation or swelling, while the solvents with significantly different solubility parameter values cannot interact with it. PTP was found to exhibit a Hildebrand solubility parameter similar to its good solvent, such as toluene (18.3). The Hildebrand solubility parameter values of ethanol, methanol and *n*-hexane are 26.2, 29.6 and 14.9, respectively. They were much closer to PTP compared with 48.0 for the water.[22,45]

As previously reported, the use of aligned MWCNTs offers a high mechanical and thermal stability.[28,30] Therefore, these composite films can be widely used as a new family of artificial materials. Herein, the use of these as a miniature crane has been demonstrated by connecting two bilayer composite films with aligned MWCNT/PTP composite films on the opposite sides of a poly (dimethylsiloxane) substrate (Fig. 6a and b). An object with a weight of 12.9 mg was suspended from the ethanol-treated composite film with two MWCNT fibers. After the ethanol was evaporated, the two bilayer composite films contract to lift up the object; the lifting distance reaches 15 mm

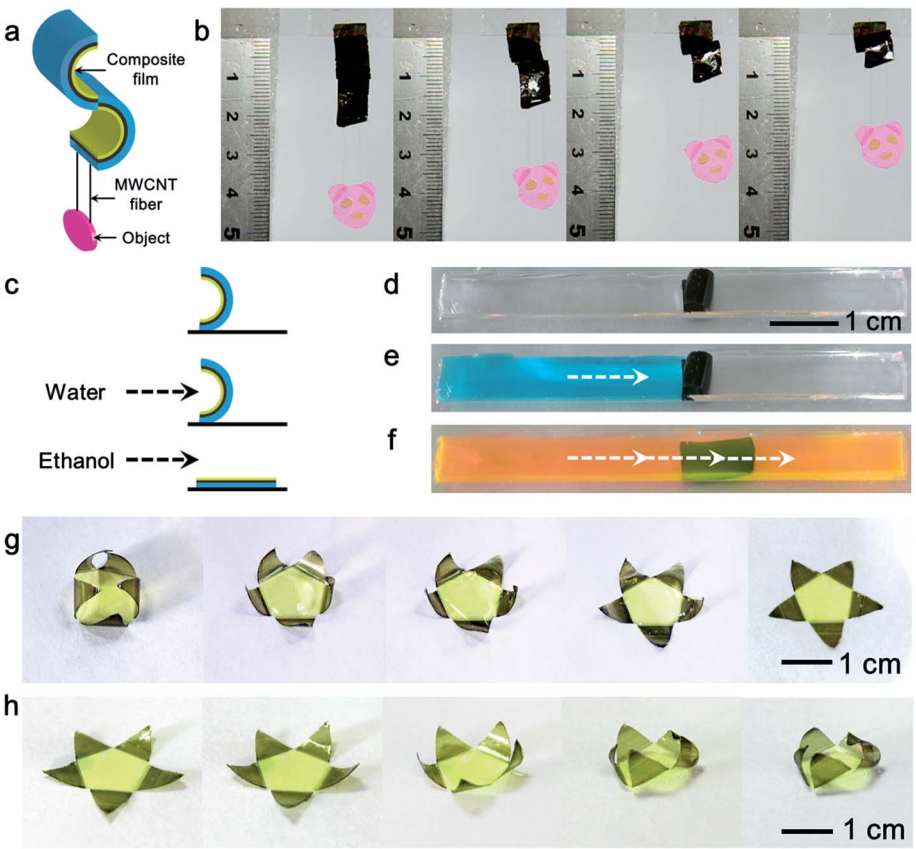

Fig. 6 (a and b) Schematic illustration and images of an object lifted due to evaporation of ethanol, respectively. The size of the film is 30 mm × 8 mm × 0.126 mm. The weight of the object is 12.9 mg. (c) Schematic illustration to a micro-valve based on the aligned MWCNT/PTP composite film. (d) Image for the experimental setup of a micro-valve. (e) Photograph for the dyed blue water being blocked by the micro-valve. (f) Image for the dyed orange ethanol passing through the micro-valve. The white arrows indicate the flowing direction. (g and h) Photographs of the reversible opening and closing processes of an artificial flower based on the aligned MWCNT/PTP composite driven by ethanol.

after the evaporation of ethanol. On absorption of ethanol in the films, the object returned to its original position. The composite film has also been used to make a micro-valve (Fig. 6c–f). One end of the curved film was fixed at the middle of a channel with the responsive aligned MWCNT/PTP composite layer towards the left. When water flows from the left, it was blocked by the curved bilayer composite film, while the ethanol can flow to the right, through the valve by unbending the film into a flat format. This micro valve can also be used in multi-channel lines to control the flowing direction of the organic solvent (Fig. S13†).

The unidirectional mechanical actuation based on solvent for the aligned MWCNT/PTP composite film could be used to efficiently design and develop complex sensors with tunable actuating behaviors. For example, the bilayer composite film was made into an artificial flower to mimic the opening and closing processes of a leaf of Venus flytrap (Fig. 6g and h). Carnivorous plant such as Venus flytrap shuts leaves to catch prey, when the shape, curvature and volume of cells change in response to the stress induced by the prey.[46] This anisotropic deformation is produced by a special arrangement of cells on the leaf surface, *i.e.*, cylindrical cells that are oriented perpendicular to rachis and cell wall is reinforced by numerous microfibrils.[46,47] Here, an artificial flower was made from five bilayer composite film petals. The MWCNTs were designed to be aligned in a direction perpendicular to the symmetry axis, providing the petals with a capability to bend towards the heart of flower. The five petals are unfolded and placed into the same plane after absorbing ethanol in 0.5 s (Fig. 6g and Movie S2†); they closed into a bud, when the ethanol evaporates (Fig. 6h and Movie S3†). As expected, the opening and closing processes of the artificial flower can be repeated for hundreds of cycles without fatigue.

Conclusion

In summary, we have developed a bilayer composite film with an aligned MWCNT/PTP composite film on isotropic poly (dimethylsiloxane) substrate that exhibits anisotropic solvent-driven bending/unbending actuation. The alignment of MWCNTs and the synergetic interaction between the MWCNTs and PTP are critical for the actuation, and the actuating direction can be well controlled at a direction perpendicular to the aligned direction of MWCNTs. The actuation has also generated an unexpected high stress of ~15 MPa that is approximately 42 times stronger than human muscle and with a good reproducibility. The reversible actuation may be repeated for 300 cycles without fatigue. These conjugated polymer composite artificial muscles are promising for a wide variety of applications such as sensors, robots and actuators. This work also represents a general and effective route in designing novel artificial muscles with high performances.

Acknowledgements

This work was supported by MOST (2011CB932503), NSFC (21225417), STCSM (12nm0503200), the Fok Ying Tong Education Foundation, the Program for Special Appointments of Professors at Shanghai Institutions of Higher Learning, and the Program for Outstanding Young Scholars from the Organization Department of the CPC Central Committee.

References

1 F. Liu and M. W. Urban, *Prog. Polym. Sci.*, 2010, **35**, 3.
2 L. Ionov, *J. Mater. Chem.*, 2010, **20**, 3382.
3 P. Brochu and Q. Pei, *Macromol. Rapid Commun.*, 2010, **31**, 10.
4 X. Zhang, C. L. Pint, M. H. Lee, B. E. Schubert, A. Jamshidi, K. Takei, H. Ko, A. Gillies, R. Bardhan, J. J. Urban, M. Wu, R. Fearing and A. Javey, *Nano Lett.*, 2011, **11**, 3239.
5 X. Yan, D. Xu, X. Chi, J. Chen, S. Dong, X. Ding, Y. Yu and F. Huang, *Adv. Mater.*, 2012, **24**, 362.
6 S. Dong, Y. Luo, X. Yan, B. Zheng, X. Ding, Y. Yu, Z. Ma, Q. Zhao and F. Huang, *Angew. Chem., Int. Ed.*, 2011, **50**, 1905.
7 M. Ma, L. Guo, D. G. Anderson and R. Langer, *Science*, 2013, **339**, 186.
8 A. Sidorenko, T. Krupenkin, A. Taylor, P. Fratzl and J. Aizenberg, *Science*, 2007, **315**, 487.
9 L. T. de Haan, J. M. N. Verjans, D. J. Broer, C. W. M. Bastiaansen and A. P. H. J. Schenning, *J. Am. Chem. Soc.*, 2014, **136**, 10585.
10 Q. Zhao, J. W. C. Dunlop, X. Qiu, F. Huang, Z. Zhang, J. Heyda, J. Dzubiella, M. Antonietti and J. Yuan, *Nat. Commun.*, 2014, **5**, 4293.
11 H. Thérien-Aubin, Z. L. Wu, Z. Nie and E. Kumacheva, *J. Am. Chem. Soc.*, 2013, **135**, 4834.
12 C. Ohm, M. Brehmer and R. Zentel, *Adv. Mater.*, 2010, **22**, 3366.
13 M. Dai, O. T. Picot, J. M. N. Verjans, L. T. de Haan, A. P. H. J. Schenning, T. Peijs and C. W. M. Bastiaansen, *ACS Appl. Mater. Interfaces*, 2013, **5**, 4945.
14 S. Ishihara, H. Wakemoto, K. Nakazima and Y. Matsuo, *Liq. Cryst.*, 1989, **4**, 669.
15 M. Kondo, Y. Yu and T. Ikeda, *Angew. Chem., Int. Ed.*, 2006, **45**, 1378.
16 G. Kwak, S. Fukao, M. Fujiki, T. Sakaguchi and T. Masuda, *Chem. Mater.*, 2006, **18**, 5537.
17 G. Kwak, M. Minakuchi, T. Sakaguchi, T. Masuda and M. Fujiki, *Chem. Mater.*, 2007, **19**, 3654.
18 G. Kwak, S. Fukao, M. Fujiki, T. Sakaguchi and T. Masuda, *Chem. Mater.*, 2006, **18**, 2081.
19 G. Kwak, W. E. Lee, H. Jeong, T. Sakaguchi and M. Fujiki, *Macromolecules*, 2009, **42**, 20.
20 M. Teraguchi and T. Masuda, *Macromolecules*, 2002, **35**, 1149.
21 W.-E. Lee, J.-W. Kim, C.-J. Oh, T. Sakaguchi, M. Fujiki and G. Kwak, *Angew. Chem., Int. Ed.*, 2010, **49**, 1406.
22 W.-E. Lee, Y.-J. Jin, L.-S. Park and G. Kwak, *Adv. Mater.*, 2012, **24**, 5604.
23 M. Moniruzzaman and K. I. Winey, *Macromolecules*, 2006, **39**, 5194.
24 H. Peng, X. Sun, F. Cai, X. Chen, Y. Zhu, G. Liao, D. Chen, Q. Li, Y. Lu, Y. Zhu and Q. Jia, *Nat. Nanotechnol.*, 2009, **4**, 738.

25 Q. Wang, Q. Yao, J. Chang and L. Chen, *J. Mater. Chem.*, 2012, **22**, 17612.
26 H. Zhao, W. Z. Yuan, L. Tang, J. Z. Sun, H. Xu, A. Qin, Y. Mao, J. K. Jin and B. Z. Tang, *Macromolecules*, 2008, **41**, 8566.
27 J. Z. Sun, A. Qin and B. Z. Tang, *Polym. Chem.*, 2013, **4**, 211.
28 X. Sun, T. Chen, Z. Yang and H. Peng, *Acc. Chem. Res.*, 2012, **46**, 539.
29 X. Sun, H. Sun, H. Li and H. Peng, *Adv. Mater.*, 2013, **25**, 5153.
30 W. Wang, X. Sun, W. Wu, H. Peng and Y. Yu, *Angew. Chem., Int. Ed.*, 2012, **51**, 4644.
31 X. Sun, Z. Zhang, X. Lu, G. Guan, H. Li and H. Peng, *Angew. Chem., Int. Ed.*, 2013, **52**, 7776.
32 K. Tsuchihara, T. Masuda and T. Higashimura, *Macromolecules*, 1992, **25**, 5816.
33 X. Sun, W. Wang, L. Qiu, W. Guo, Y. Yu and H. Peng, *Angew. Chem., Int. Ed.*, 2012, **51**, 8520.
34 H. Peng, *J. Am. Chem. Soc.*, 2007, **130**, 42.
35 R. Pelrine, R. Kornbluh, J. Joseph, R. Heydt, Q. Pei and S. Chiba, *Mater. Sci. Eng., C*, 2000, **11**, 89.
36 T. Mirfakhrai, J. D. W. Madden and R. H. Baughman, *Mater. Today*, 2007, **10**, 30.
37 K. Kaneto, H. Suematsu and K. Yamato, *Bioinspiration Biomimetics*, 2008, **3**, 035005.
38 B.-G. Kim, E. J. Jeong, J. W. Chung, S. Seo, B. Koo and J. Kim, *Nat. Mater.*, 2013, **12**, 659.
39 B. McCarthy, J. N. Coleman, R. Czerw, A. B. Dalton, M. in het Panhuis, A. Maiti, A. Drury, P. Bernier, J. B. Nagy, B. Lahr, H. J. Byrne, D. L. Carroll and W. J. Blau, *J. Phys. Chem. B*, 2002, **106**, 2210.
40 D. Lee, Y.-J. Jin, H. Kim, N. Suzuki, M. Fujiki, T. Sakaguchi, S. K. Kim, W.-E. Lee and G. Kwak, *Macromolecules*, 2012, **45**, 5379.
41 Z. Chen, V. Augustyn, J. Wen, Y. Zhang, M. Shen, B. Dunn and Y. Lu, *Adv. Mater.*, 2011, **23**, 791.
42 N. G. Sahoo, H. K. F. Cheng, L. Li, S. H. Chan, Z. Judeh and J. Zhao, *Adv. Funct. Mater.*, 2009, **19**, 3962.
43 M. Jamal, A. M. Zarafshar and D. H. Gracias, *Nat. Commun.*, 2011, **2**, 527.
44 W.-E. Lee, D.-C. Han, D.-H. Han, H.-J. Choi, T. Sakaguchi, C.-L. Lee and G. Kwak, *Macromol. Rapid Commun.*, 2011, **32**, 1047.
45 D.-C. Han, Y.-J. Jin, J.-H. Lee, S.-I. Kim, H.-J. Kim, K.-H. Song and G. Kwak, *Macromol. Chem. Phys.*, 2014, **215**, 1068.
46 Y. Forterre, J. M. Skotheim, J. Dumais and L. Mahadevan, *Nature*, 2005, **433**, 421.
47 D. H. Gracias, *Curr. Opin. Chem. Eng.*, 2013, **2**, 112.

